

## Liquid Phase Sintering of Silicon Carbide with AlN/Y<sub>2</sub>O<sub>3</sub>, Al<sub>2</sub>O<sub>3</sub>/Y<sub>2</sub>O<sub>3</sub> and SiO<sub>2</sub>/Y<sub>2</sub>O<sub>3</sub> Additions

*Kurt Strecker<sup>a</sup>, Sebastião Ribeiro<sup>a</sup>, Daniela Camargo<sup>a</sup>, Rui Silva<sup>b\*</sup>,  
Joaquim Vieira<sup>b</sup>, Filipe Oliveira<sup>b</sup>*

<sup>a</sup>*Faculdade de Engenharia Química de Lorena, Departamento de Engenharia de  
Materiais, C.P. 116, 12600-000 Lorena - SP, Brazil*

<sup>b</sup>*Universidade de Aveiro, Departamento de Cerâmica e Vidro, 3810 Aveiro, Portugal*

Received: January 20, 1999 Revised: August 3, 1999

In this work, the influence of the additive system on the liquid phase sintering of silicon carbide has been investigated. The additives employed were mixtures of AlN/Y<sub>2</sub>O<sub>3</sub>, Al<sub>2</sub>O<sub>3</sub>/Y<sub>2</sub>O<sub>3</sub> and SiO<sub>2</sub>/Y<sub>2</sub>O<sub>3</sub>. The total additive content was fixed at 20 vol.-%, maintaining the Y<sub>2</sub>O<sub>3</sub> content in each additive system at 35 vol.-%. Cold isostatically pressed samples were sintered at 1900, 2000 and 2100 °C under Ar atmosphere during 30min. The most promising results have been obtained by samples with AlN/Y<sub>2</sub>O<sub>3</sub> additions sintered at 2000 °C, exhibiting the smallest weight loss of about 6% and the highest flexural strengths of about 433 MPa. Samples with Al<sub>2</sub>O<sub>3</sub>/Y<sub>2</sub>O<sub>3</sub> and SiO<sub>2</sub>/Y<sub>2</sub>O<sub>3</sub> additions exhibited high weight loss, because of reactions of Al<sub>2</sub>O<sub>3</sub> and SiO<sub>2</sub> with the SiC matrix, forming gaseous species such as Al<sub>2</sub>O, SiO and CO, resulting in depletion of the liquid phase, and, consequently, in inferior final densities and mechanical properties. Concerning the SiO<sub>2</sub>/Y<sub>2</sub>O<sub>3</sub> additive system, the reactions seem to be completed already at temperatures below 1900 °C, turning this additive mixture unsuitable. The microstructural analysis indicated only the presence of the β-SiC phase for all samples; no phase transformation of the β-SiC into α-SiC has been observed.

**Keywords:** *silicon carbide, liquid phase sintering, microstructure*

### 1. Introduction

Silicon carbide, SiC, is a covalent compound of low density, high hardness, high thermal stability – decomposition occurs at 2300 °C – and good thermal conductivity, resulting in a good thermal shock resistance. Furthermore, SiC is relatively stable in aggressive environment. Because of these properties SiC ceramics is widely used in refractories and heat exchangers. Other applications include abrasives and heating elements. Only its relatively low fracture toughness is a limiting factor for a wider range of applications as a structural ceramic.

Due to its covalent nature of bonding, the production of dense, monolithic SiC ceramics without sintering aids is impossible. The most common additives used are small quantities of C and B or Al and their compounds, such as B<sub>4</sub>C<sup>1-4</sup>. In such way it is possible to densify SiC at temperatures between 2100 and 2300 °C up to 99%. The materials obtained – denominated SSiC (sintered silicon carbide) – consist basically of α-SiC grains without an intergranular

phase and due to the strong interfacial bonding of the grains a transcrystalline fracture mode prevails, resulting in a low fracture toughness of about 3 - 4 MPa m<sup>1/2</sup>.

In the last decade were considered the liquid phase sintering of SiC, using oxide mixtures as additives<sup>5-9</sup>. These materials, called LPS-SiC (liquid phase sintered silicon carbide), can be densified at temperatures below 2100 °C. Besides a lower sintering temperature, the LPS-SiC materials exhibit another interesting aspect as compared to SSiC, which is that the fracture toughness can be increased by the control of the phase transformation of β-SiC into α-SiC, leading to elongated α-SiC grains formation and resulting in situ reinforcement, similar to Si<sub>3</sub>N<sub>4</sub> ceramics<sup>10</sup>. The mechanisms contributing to the increase of the fracture toughness are crack deflection and crack bridging<sup>11</sup>, caused by the microstructural modifications, as well as internal stresses created by the different thermal expansion coefficients of the SiC matrix and the secondary intergranular phase<sup>12</sup>.

Even though the majority of the published works report the use of  $\text{Al}_2\text{O}_3/\text{Y}_2\text{O}_3$  mixtures as sintering additives, other compounds can be also used as sintering aids, as shown by K. Negita<sup>13</sup>. However, weight loss due to the evaporation of the additives remains a major problem in liquid phase sintering of SiC ceramics.

The principal objective of the present work is to compare the influence of the additive systems  $\text{AlN}/\text{Y}_2\text{O}_3$ ,  $\text{Al}_2\text{O}_3/\text{Y}_2\text{O}_3$  and  $\text{SiO}_2/\text{Y}_2\text{O}_3$  on the liquid phase sintering of SiC ceramics, the microstructure and the mechanical properties.

## 2. Experimental

The starting powders used in this study were  $\beta$ -SiC B20,  $\text{Y}_2\text{O}_3$  Grade Fine and AlN all by H. C. Starck and  $\text{SiO}_2$  of Merck. Three powder mixtures with three different combinations of sintering additives,  $\text{AlN}/\text{Y}_2\text{O}_3$ ,  $\text{Al}_2\text{O}_3/\text{Y}_2\text{O}_3$  and  $\text{SiO}_2/\text{Y}_2\text{O}_3$ , were prepared by attrition milling in isopropilic alcohol. The additive content was fixed at 20 vol.-% of the total mixture and the  $\text{Y}_2\text{O}_3$  content in the additive systems was kept constant at 35 vol.-%. The overall compositions of the different powder mixtures as well as their denominations are presented in Table 1.

After homogenization, the powder mixtures were dried in a rotoevaporator and deagglomerated by sieving. Particle size distribution was measured by sedigraphy (SYM-PATEC HELOS). Samples of approximately  $4 \times 4 \times 50 \text{ mm}^3$  were pressed first uniaxially under 20 MPa and then isostatically under 300 MPa. Green density of the pressed samples were determined.

The samples were sintered in a furnace with a graphite heating element under Ar atmosphere, using graphite crucibles and SiC powder as powder bed. The heating rate employed was 10 K/min up to the maximum sintering temperatures of 1900, 2000 and 2100 °C, with a holding time of 30 min. The cooling rate has been the same until the inertia of the furnace prevailed.

The sintered samples were characterized for final density determined by the Archimedes method, weight loss during sintering and linear shrinkage. Prior to the mechanical and microstructural characterization, the samples were grinded and polished with diamond paste. Phase analysis was accomplished by X-ray diffraction, using  $\text{CuK}\alpha$ -radiation. Young's modulus was determined by the acoustic resonance method, and the Vickers hardness was deter-

mined under a load of 9.81 N. Strength was evaluated by the 3-point flexural strength measurements.

Microstructural characterization by scanning electron microscopy (SEM) was conducted on fracture surfaces and on polished surfaces using backscattered electrons in order to obtain the necessary contrast between the SiC grains and the intergranular phase. Relative contents of Y, Al and Si of samples sintered at 2100 °C were determined by EDS analysis.

## 3. Results and Discussion

Figure 1 shows the particle size distributions of the three different powder mixtures prepared by attrition milling. The average particle size of all three powders is about 0.75  $\mu\text{m}$ . The distribution curves are very similar, indicating the efficiency of attrition milling and the homogeneity of the three powder mixtures prepared.

The green, theoretical and relative densities of the compacted samples prior to sintering are resumed in Table 2. The calculations of the theoretical density were based on the rule of mixtures.

The results of the weight loss ( $\Delta m/m_0$ ) during sintering, linear shrinkage ( $\Delta l/l_0$ ), and final relative densities ( $\rho_{rel}$ ) of the sintered samples are presented graphically in Figs. 2 - 4. As it can be seen, the samples with  $\text{Al}_2\text{O}_3/\text{Y}_2\text{O}_3$  and  $\text{SiO}_2/\text{Y}_2\text{O}_3$  additions suffer extremely high weight loss of up to 19.7 and 15.5%, respectively at the sintering temperature of 2100 °C. This may be explained by the interaction between silicon carbide and the additives resulting in gase-

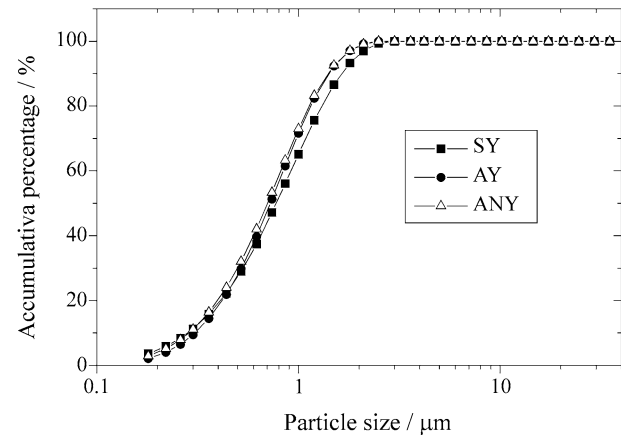


Figure 1. Particle size distribution of the powder mixtures.

Table 1. Denomination and composition of the powder mixtures prepared.

Powder Mixture	Denomination	Composition (wt.-%)				
SiC - $\text{AlN}/\text{Y}_2\text{O}_3$ , ANY	76.80	12.79	-	-	10.41	
SiC - $\text{Al}_2\text{O}_3/\text{Y}_2\text{O}_3$	AY	74.69	-	15.19	-	10.12
SiC - $\text{SiO}_2/\text{Y}_2\text{O}_3$	SY	80.16	-	-	8.97	10.87

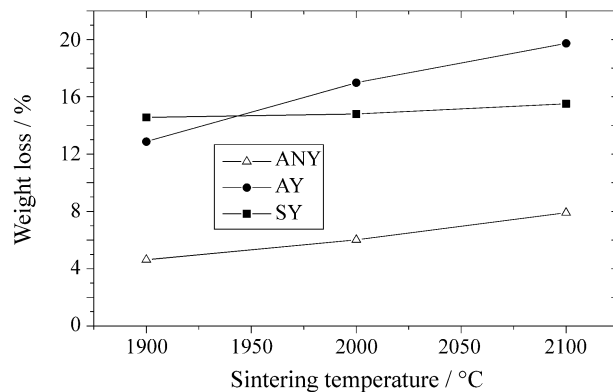
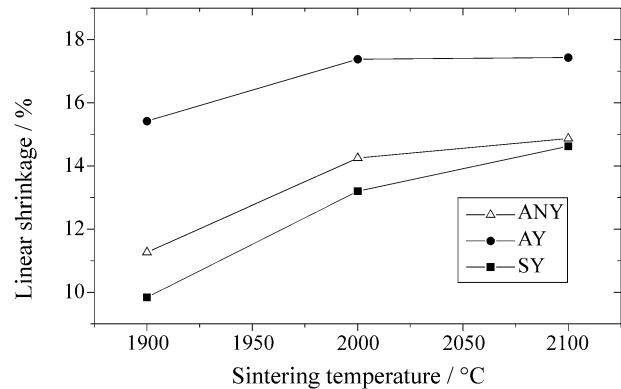
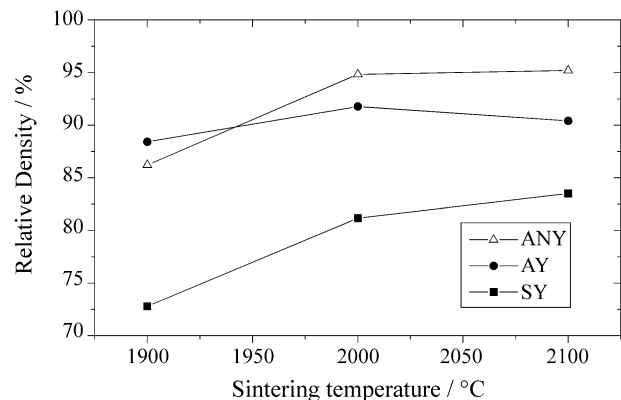
**Table 2.** Green density, theoretical density and relative green density of the compacted samples.

Sample	Theoretical density [ $\text{g}/\text{cm}^3$ ]	Green density [ $\text{g}/\text{cm}^3$ ]	Relative green density [%]
ANY	3.294	2.07	63.04
AY	3.404	2.07	60.63
SY	3.102	1.95	63.01

ous species formation, such as  $\text{SiO}$ ,  $\text{Al}_2\text{O}$ ,  $\text{CO}$  and  $\text{CO}_2$ <sup>14,15</sup>. In the case of  $\text{SiO}_2/\text{Y}_2\text{O}_3$  additions the reactions seem to be completed below  $1900^\circ\text{C}$ , as can be concluded by the almost constant weight loss at all sintering temperatures (Fig. 2). In the case of  $\text{Al}_2\text{O}_3$  additions the reactions proceed up to  $2100^\circ\text{C}$ , causing a constant increase of weight loss. The higher weight losses observed for the AY samples in relation to the SY samples are due to the higher initial  $\text{Al}_2\text{O}_3$  weight content in comparison to the initial  $\text{SiO}_2$  content (Table 1). On the other hand, samples with the  $\text{AlN}/\text{Y}_2\text{O}_2$  additive system exhibited only minor weight loss, thus maintaining a higher liquid phase content during sintering. These findings are confirmed by EDS analysis of polished surfaces, as shown in Table 3, where the normalized relative contents of Si, Al and Y in the starting powder mixtures (calculated) and after sintering at  $2100^\circ\text{C}$  are listed.

Although the O and C contents could not be analyzed by this method and although these analysis do not represent an overall quantitative analysis of the samples, the trends described above are confirmed, *i.e.* the Si and Al contents diminish due to the reactions between  $\text{SiO}_2$  and  $\text{Al}_2\text{O}_3$  with  $\text{SiC}$ , leading to an increase of the Y content. Higher loss of Al is observed for  $\text{Al}_2\text{O}_3/\text{Y}_2\text{O}_3$  system in comparison with the  $\text{AlN}/\text{Y}_2\text{O}_3$  one, which is in agreement with the weight loss presented in Fig. 2. Si loss was highest for the SY samples.

As it can be seen from Figs. 3 and 4, the highest densification was achieved for the samples with  $\text{AlN}/\text{Y}_2\text{O}_3$  additives, sintered at  $2000$  and  $2100^\circ\text{C}$ , although they exhibited a smaller linear shrinkage as the samples with  $\text{Al}_2\text{O}_3/\text{Y}_2\text{O}_3$  additives. For the samples sintered at  $1900^\circ\text{C}$ , the highest density was achieved by samples with

**Figure 2.** Weight loss of the samples vs. sintering temperature.**Figure 3.** Linear shrinkage of the samples vs. sintering temperature.**Figure 4.** Relative density of the samples vs. sintering temperature.

$\text{Al}_2\text{O}_3/\text{Y}_2\text{O}_3$  additives. This behavior can be explained by the higher refractoriness of the  $\text{AlN}$  as compared to  $\text{Al}_2\text{O}_3$ , which therefore needs higher sintering temperatures for complete densification. In the case of the SY samples, the linear shrinkage as well as the final relative densities are significantly lower as compared with other samples due to the loss of  $\text{SiO}_2$  additive at temperatures below  $1900^\circ\text{C}$ .

Considering all these observations, it can be concluded that the  $\text{AlN}/\text{Y}_2\text{O}_3$  additive system is the most adequate for the liquid phase sintering of  $\text{SiC}$  ceramics. The weight losses might be reduced even further by the use of an appropriate powder bed. A sintering temperature of  $2000^\circ\text{C}$  is sufficient to obtain high densification, while higher temperatures cause lower final densities due to increasing weight loss caused by evaporation of the addi-

**Table 3.** Relative content of Si, Al and Y in the starting powders (calculated) and after sintering at 2100 °C (determined by EDS analysis).

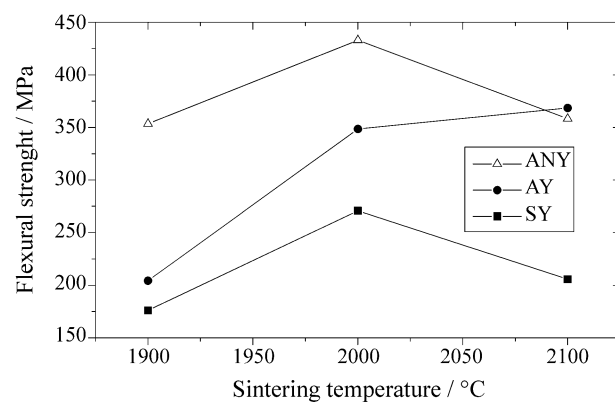
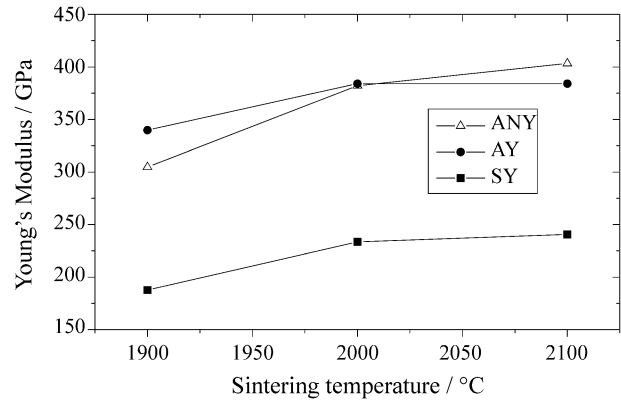
Sample	Initial normalized content (wt.-%)	Final normalized content (wt.-%)
ANY	Si 76.39	Si 71.05
	Al 11.97	Al 10.01
	Y 11.64	Y 18.94
AY	Si 76.39	Si 74.50
	Al 11.77	Al 6.45
	Y 11.67	Y 19.05
SY	Si 87.63	Si 80.93
	Y 12.37	Y 19.07

tives. Furthermore, the final densities might be improved by longer sintering time.

The results of the Young's modulus  $E$ , Vickers hardness HV1 and flexural strength measurements are presented in Figs. 5 and 6, respectively. Due to the high porosity of the samples with  $\text{SiO}_2/\text{Y}_2\text{O}_3$  additions no meaningful hardness measurements were possible.

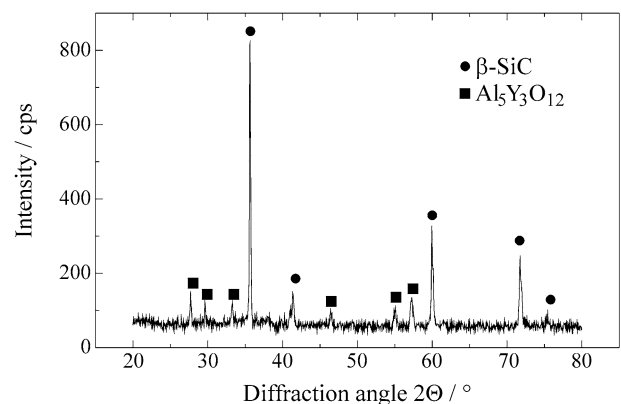
As can be observed in Fig. 5, the samples with  $\text{AlN}/\text{Y}_2\text{O}_3$  additions reach their highest flexural strengths of about 430 MPa after sintering at 2000 °C. The other two materials had lower flexural strength, due to their lower final densities. The Young's modulus values plotted vs. sintering temperature in Fig. 6 exhibit similar trends to the ones of the final density of the sintered samples, demonstrating the direct influence of porosity on the elastic behavior.

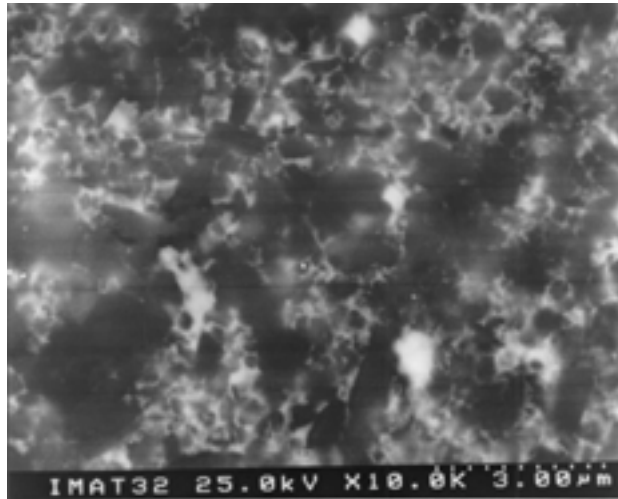
The phase analysis of the sintered samples at 2100 °C by X ray diffraction revealed only the  $\beta$ -SiC phase in all cases. Trace amounts of the  $\text{Al}_5\text{Y}_3\text{O}_{12}$  phase appeared in the case of  $\text{Al}_2\text{O}_3$  and  $\text{AlN}$  additions. No secondary crystalline phase was identified in the case of  $\text{SiO}_2$  additions. Figure 7 shows a X-ray diffractogram of a sample with  $\text{Al}_2\text{O}_3/\text{Y}_2\text{O}_3$  additions sintered at 2100 °C. No phase trans-

**Figure 5.** Flexural strength of the samples vs. sintering temperature.**Figure 6.** Young's modulus of the sintered samples vs. sintering temperature.

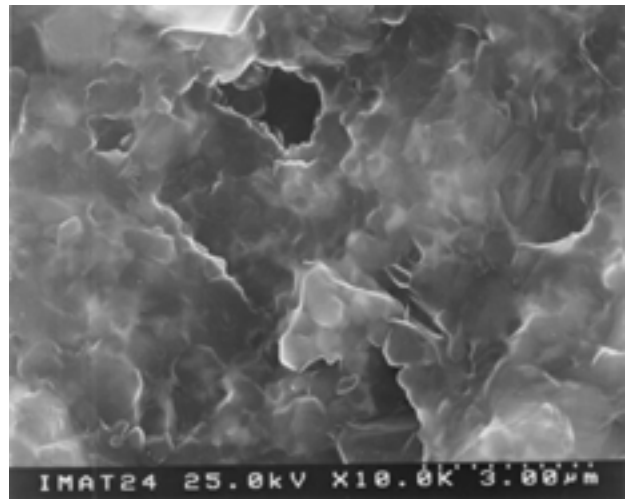
formation of  $\beta$ -SiC into  $\alpha$ -SiC has been observed, probably due to the high purity in terms of the initial  $\alpha$ -SiC phase content of the SiC starting powder and due to the short sintering time of only 30 min.

The microstructures of polished and fracture surfaces of the samples sintered at 2100 °C are shown in Fig. 8. In the case of  $\text{AlN}/\text{Y}_2\text{O}_3$  and  $\text{Al}_2\text{O}_3/\text{Y}_2\text{O}_3$  quite similar microstructures are observed. Both exhibit a fine grained microstructure of equiaxial SiC grains with grain size smaller than 2  $\mu\text{m}$ . No exaggerated grain growth or typically elongated  $\alpha$ -SiC grains have been observed, being in agreement with the results of the X ray analysis. In comparison, the samples with  $\text{SiO}_2/\text{Y}_2\text{O}_3$  additions exhibit significant grain growth in relation to the other two compositions, with grain sizes between 3 to 5  $\mu\text{m}$ . Again, no phase transformation of  $\beta$ -SiC into  $\alpha$ -SiC has been observed in this case. The fracture surfaces are quite smooth, indicating a predominantly transcrystalline fracture mode, leading to low fracture toughness. No definitive conclusion can be drawn in the case of the  $\text{SiO}_2/\text{Y}_2\text{O}_3$  doped samples, because of their very low densities.

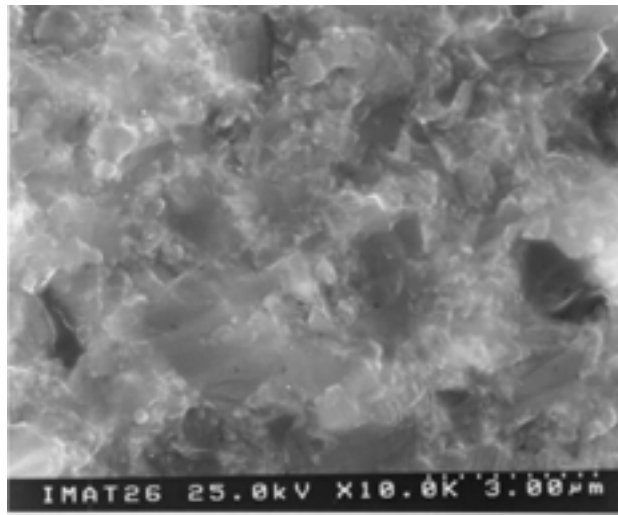
**Figure 7.** X-ray diffractogram of a SiC- $\text{Al}_2\text{O}_3/\text{Y}_2\text{O}_3$  sample sintered at 2100 °C.



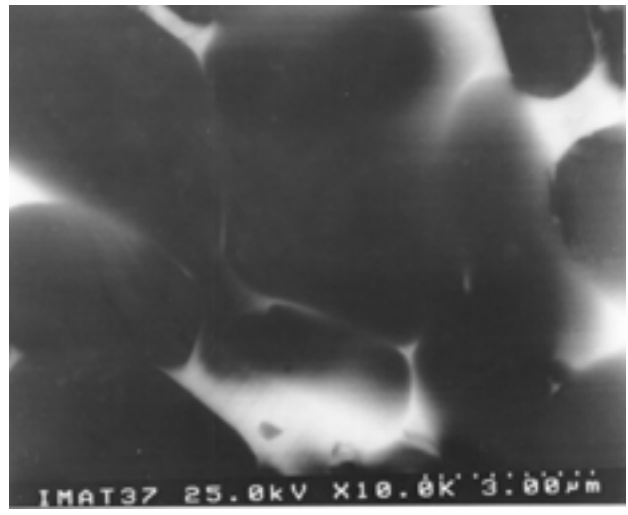
a) ANY



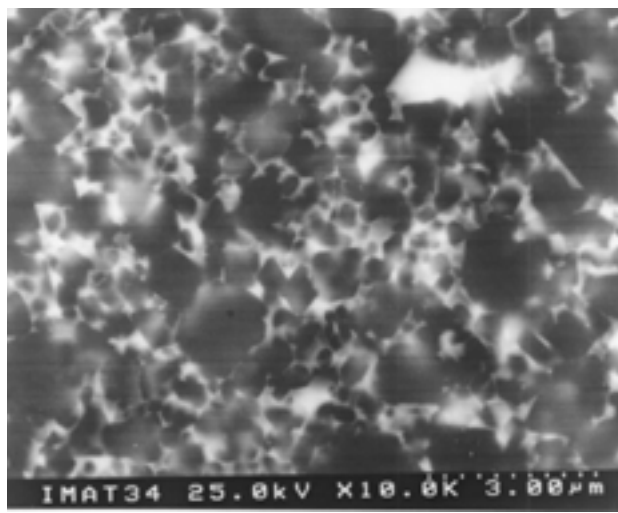
d) AY



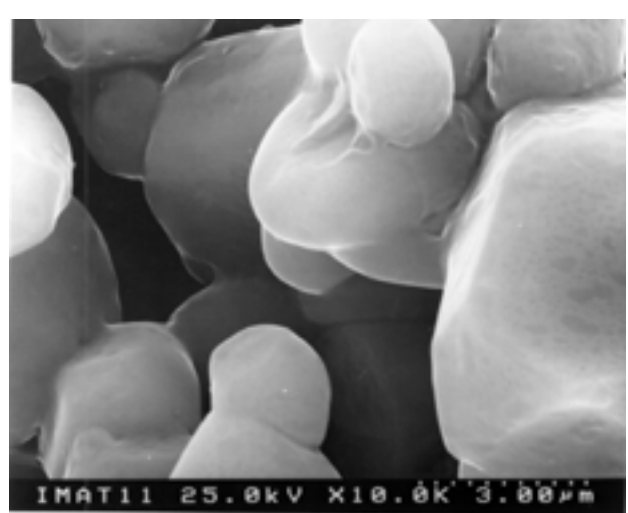
b) ANY



e) SY



c) AY



f) SY

**Figure 8.** Microstructures (left) and fracture surfaces (right) of the samples sintered at 2100 °C, with additions of AlN/Y<sub>2</sub>O<sub>3</sub> (a, b), Al<sub>2</sub>O<sub>3</sub>/Y<sub>2</sub>O<sub>3</sub> (c, d) and SiO<sub>2</sub>/Y<sub>2</sub>O<sub>3</sub> (e, f).

## 4. Conclusions

Considering the results presented, it is concluded that the additive system based on the AlN/Y<sub>2</sub>O<sub>3</sub> mixture is the most adequate for the liquid phase sintering of SiC. Due to the higher refractoriness of AlN, in relation to Al<sub>2</sub>O<sub>3</sub>, samples with AlN addition reach the highest densities at higher sintering temperatures. The weight losses of these samples might be reduced using powder beds with identical compositions, resulting in higher densities and hence in improvement of mechanical properties. The SiO<sub>2</sub>/Y<sub>2</sub>O<sub>3</sub> system is inadequate for the liquid phase sintering of SiC ceramics, due to the SiO<sub>2</sub> loss at low temperatures.

The fact that no β-SiC to α-SiC phase transformation has been observed, may be explained by the short sintering time of only 30 min and by the absence of α-SiC grains in the starting powder, which hinders the nucleation of the α-SiC phase. To induce the phase transition of β-SiC into α-SiC a prolonged heat treatment or the use of α-SiC seeds seems to be necessary.

In the case of the SiO<sub>2</sub>/Y<sub>2</sub>O<sub>3</sub> additive system, an intensive grain growth has been observed as compared to the two other additive systems investigated. The high porosity of this samples indicates that the grain growth probably occurs via an evaporation – condensation mechanism.

Considering the final relative density of about 95% of the samples with AlN/Y<sub>2</sub>O<sub>3</sub> additions and their flexural strengths of about 430 MPa, the high potential of LPS-SiC as a structural ceramic material was demonstrated in this work.

## Acknowledgement

The authors would like to thank the financial support by CAPES-ICCTI under grant no. 019/97 and by FAPESP under grant no. 95/06378-5.

## References

1. Prochazka, S. *Proceedings of the Conference on Ceramics for High Performance Applications*, Hyanuis, MA, 1973. Burke, J.J.; Gorum, A.E.; Katz, R.M., eds., Brook Hill Publishing Co., p. 7-13, 1975.
2. Prochazka, S. *Special Ceramics 6, British Ceramic Res. Assoc., Stoke-on-Trent*, p. 171-181, 1975.
3. Johnson, C.A., Prochazka, S. *Ceramic Microstructures '76*, edited by Fulrath and Park, p. 366-378, 1977.
4. Murata, Y.; Smoak, R.H. *Proceedings of the International Symposium of Factors in Densification and Sintering of Oxide and Non-oxide Ceramics*, October 3-6, Hakone, Japão, p. 382-399, 1978.
5. Cutler, R.A.; Jackson, T.B. *Ceramic Materials and Components for Engines. Proceedings of the Third International Symposium*. Tennery, V.J., ed., The American Ceramic Society, Westerville, OH, p. 309-318, 1989.
6. Cordery, L.; Niesz, D.E.; Shanefield, D. J. *Sintering of Advanced Ceramics*, v. 7, Handwerker, C.A.; Blendell, J.E.; Kaysser, W.A., eds., The American Ceramic Society, Westerville, OH, p. 618-636, 1990.
7. Kim, D.H., Kim, C.H. *J. Am. Ceram. Soc.*, v. 73, n. 5, p. 1431-1434, 1990.
8. Chia, K.Y., Lau, S.K. *Ceram. Eng. Sci. Proc.*, v. 12, n. 9-10, p. 1845-1861, 1991.
9. Kim, Y.W. *et al. J. Am. Ceram. Soc.*, v. 78, n. 11, p. 3145-3148, 1995.
10. Tani, E. *et al. J. Am. Ceram. Bull.*, v. 65, n. 9, p. 1311-1315, 1986.
11. Lee, S.K. *et al. J. Am. Ceram. Soc.*, v. 78, n. 1, p. 65-70, 1995.
12. Padture, N.P. *J. Am. Ceram. Soc.*, v. 77, n. 2, p. 519-523, 1994.
13. Negita, K. *J. Am. Ceram. Soc.*, v. 69, p. C-308 - C-310, 1986.
14. Jacobson, N.S. *J. Am. Ceram. Soc.*, v. 75, p. 1603-1611, 1992.
15. Hue, F.; Yorand, Y.; Dubois, J.; Fantozzi, G. *J. Europ. Ceram. Soc.*, v. 17, p. 557-563, 1997.